

Correlated two-photon scattering in cavity optomechanics

Jie-Qiao Liao^{1,2} and C. K. Law¹

¹*Department of Physics and Institute of Theoretical Physics, The Chinese University of Hong Kong, Shatin, Hong Kong Special Administrative Region, People's Republic of China*

²*Center for Emergent Matter Science, RIKEN, Wako-shi, Saitama 351-0198, Japan*

(Dated: April 11, 2013)

We present an exact analytical solution of the two-photon scattering in a cavity optomechanical system. This is achieved by solving the quantum dynamics of the total system, including the optomechanical cavity and the cavity-field environment, with the Laplace transform method. The long-time solution reveals detailed physical processes involved as well as the corresponding resonant photon frequencies. We characterize the photon correlation induced in the scattering process by calculating the two-photon joint spectrum of the long-time state. Clear evidence for photon frequency anti-correlation can be observed in the joint spectrum. In addition, we calculate the equal-time second-order correlation function of the cavity photons. The results show that the radiation pressure coupling can induce photon blockade effect, which is strongly modulated by the phonon sideband resonance. In particular, we obtain an explicit expression of optomechanical coupling strength determining these sideband modulation peaks based on the two-photon resonance condition.

PACS numbers: 42.50.Pq, 42.50.Wk, 42.50.Ar, 07.10.Cm

I. INTRODUCTION

The realization of photon-photon interaction at few-photon level has been a research subject of major interest in quantum optics [1, 2]. The significance of few-photon interaction exists not only for studying the foundations of quantum theory, but also for applications in quantum information science. Specifically, an important goal in the current field of research is the control of two-photon correlations. Such a problem has been discussed in various nonlinear systems [3–9]. For example, it has been shown that photon-photon interaction can be achieved in nonlinear Kerr media, and interesting quantum correlation effects such as photon blockade [1, 2, 10] appear in the strong-coupling regime. In particular, a strong Kerr nonlinearity can be achieved through the interaction between light and atoms [1, 2].

Interestingly, an optomechanical cavity [11–13] driven by radiation-pressure can be mapped to a problem with a Kerr-type interaction [14–16], and hence provides a different class of systems to explore phenomena of interacting photons through the control of mechanical motion of the cavity mirrors. Indeed, Rabl [17] has examined the photon blockade effect in a continuously driven cavity optomechanical system operated in the single-photon strong-coupling regime. In such a regime, a single cavity photon can significantly change the resonant frequency of the cavity field and leads to a range of interesting effects, such as quantum state preparation [14, 15, 18, 19], multiple mechanical sidebands [20], scattering [21], single-photon cooling [22], and optomechanical instability [23]. We note that several recent experimental systems in cavity optomechanics [24–26] are approaching the single-photon strong-coupling regime.

In this paper, we investigate the quantum dynamics of a photon pair interacting with a moving mirror in a

cavity. Different from previous studies [17, 20] in which a continuously driven system is treated perturbatively, our system confined in the two-photon subspace is exactly solvable and therefore provides a fundamental configuration to study how two photons can become correlated via optomechanical coupling. We shall focus on the scattering problem in which a two-photon wave packet is injected into the cavity. By treating the cavity field, the moving mirror, and the field continuum outside the cavity as a whole system, we can solve the quantum state evolution via the Wigner-Weisskopf method. From the long-time solution, we identify quantitatively the probability amplitudes associated with various scattering processes inside the cavity.

We emphasize that our exact solution provides a complete description of the full quantum state, including the system's environment, and this is not directly attainable in previous related studies based on the master equation of the system's reduced density matrix [27] or approximated operator solutions in Heisenberg's picture [17]. The knowledge of the full quantum state enables us to learn about the details of underlying physical processes as well as the quantum structure of interacting photons in optomechanical cavities. In this paper, we also calculate the joint spectrum of the two scattered photons. From the joint spectrum, we can see clear evidence for the photon frequency anti-correlation, which is a qualitative evaluation of the two-photon correlation. In addition, we calculate the equal-time second-order correlation function of the cavity photons at transient times as a quantitative measurement of the two-photon correlation. The results indicate that photon blockade is strongly modulated by the optomechanical coupling strength as well as the Franck-Condon factors involved. More importantly, we find out the explicit modulation rule of the optomechanical coupling strength based on the two-photon res-

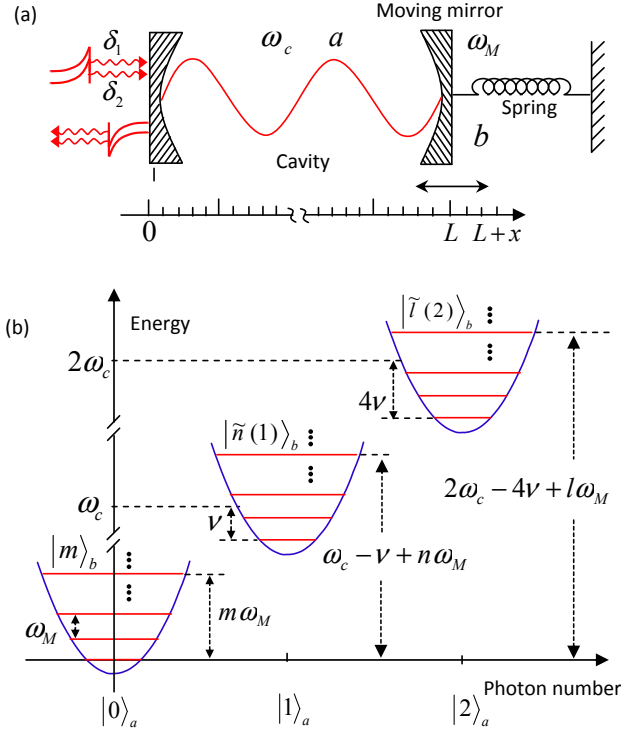


FIG. 1: (Color online) (a) Schematic diagram of a Fabry-Pérot-type optomechanical cavity formed by a fixed end mirror and a moving end mirror. (b) The energy-level structure (unscaled) of the optomechanical cavity (limited in the zero-, one-, and two-photon subspaces).

onance.

II. THE MODEL

The system under consideration is a Fabry-Pérot-type optomechanical cavity formed by a fixed end mirror and a moving end mirror [see Fig. 1(a)]. We focus on a single-mode cavity field, which is coupled to the mechanical oscillation of the moving mirror via radiation pressure. The moving end mirror is assumed to be perfect and the fixed one is partially transparent. In a rotating frame defined by the unitary transformation $e^{-iN\omega_c t}$ with $N = a^\dagger a + \int_0^\infty c_k^\dagger c_k dk$ being the total photon number operator, the Hamiltonian of the whole system including the optomechanical cavity and the environment reads as

$$H_I = \hbar\omega_M b^\dagger b - \hbar g_0 a^\dagger a (b^\dagger + b) + \int_0^\infty \hbar \Delta_k c_k^\dagger c_k dk + \hbar \xi \int_0^\infty (c_k^\dagger a + a^\dagger c_k) dk. \quad (1)$$

Here a (a^\dagger) and b (b^\dagger) are, respectively, the annihilation (creation) operators of the cavity field and the moving mirror, with the respective frequencies ω_c and ω_M . c_k (c_k^\dagger) is the annihilation (creation) operator of the continuous field mode k outside the cavity with the resonant fre-

quency ω_k ($\Delta_k = \omega_k - \omega_c$ is the detuning). The radiation-pressure coupling appearing in the second term of H_I is characterized by the coupling strength g_0 , and the coupling between the cavity field and the outside fields is modeled by the hopping interaction with the coupling strength $\xi = \sqrt{\gamma_c/2\pi}$ (γ_c is the cavity-field decay rate). Since the decay rate of the mechanical resonator γ_M can be much smaller than γ_c , we will neglect the dissipation of the mechanical resonator in our discussions. This is justified as long as the scattering processes are completed in a time much shorter than γ_M^{-1} .

In this paper, we will focus on the two-photon scattering problem. Because the total photon number is a conserved quantity, the Hilbert space for the photon part in this problem is spanned by three types of basis vectors: $|2\rangle_a|\emptyset\rangle$, $|1\rangle_a|1_k\rangle$, and $|0\rangle_a|1_p, 1_q\rangle$, where $|2\rangle_a|\emptyset\rangle$ stands for the state with two photons in the cavity and the outside fields are in a vacuum, $|1\rangle_a|1_k\rangle$ represents the state with one photon in the cavity, one photon in the k mode of the outside fields, and the state $|0\rangle_a|1_p, 1_q\rangle$ means that there is no photon in the cavity, two photons are in the p and q modes of the outside fields. By using these basis vectors for the fields, the state vector of the total system at time t is denoted by

$$|\Phi(t)\rangle = \sum_{m=0}^{\infty} A_m(t) |2\rangle_a |\emptyset\rangle |\tilde{m}(2)\rangle_b + \sum_{m=0}^{\infty} \int_0^\infty dk B_{m,k}(t) |1\rangle_a |1_k\rangle |\tilde{m}(1)\rangle_b + \sum_{m=0}^{\infty} \int_0^\infty dp \int_0^\infty dq C_{m,p,q}(t) |0\rangle_a |1_p, 1_q\rangle |m\rangle_b$$

where we have introduced the single- and two-photon displaced number states for the moving mirror

$$|\tilde{m}(1)\rangle_b \equiv e^{\beta_0(b^\dagger - b)} |m\rangle_b, \quad |\tilde{m}(2)\rangle_b \equiv e^{2\beta_0(b^\dagger - b)} |m\rangle_b, \quad (3)$$

with $\beta_0 \equiv g_0/\omega_M$ being the single-photon displacement quantity. We note that these displaced number states are eigenstates of the Hamiltonian

$$H_{\text{opc}} = \hbar\omega_c a^\dagger a + \hbar\omega_M b^\dagger b - \hbar g_0 a^\dagger a (b^\dagger + b) \quad (4)$$

of the optomechanical cavity, as defined by the eigen-equation

$$H_{\text{opc}} |l\rangle_a |\tilde{m}(l)\rangle_b = \hbar(l\omega_c + m\omega_M - l^2\nu) |l\rangle_a |\tilde{m}(l)\rangle_b, \quad (5)$$

where $\nu \equiv g_0^2/\omega_M$ is the single-photon-state frequency shift. The energy-level structure limited in the zero-, one-, and two-photon subspaces of the optomechanical cavity is shown in Fig. 1(b).

Based on Eqs. (1), (2), and the Schrödinger equation, we obtain the following equations of motion for probabilities

$$\dot{A}_m(t) = -i(m\omega_M - 4\nu)A_m(t) - i\sqrt{2}\xi \sum_{n=0}^{\infty} \int_0^{\infty} \langle \tilde{m}(2)|_b |\tilde{n}(1)\rangle_b B_{n,k}(t) dk, \quad (6a)$$

$$\dot{B}_{m,k}(t) = -i(\Delta_k - \nu + m\omega_M)B_{m,k}(t) - i\sqrt{2}\xi \sum_{n=0}^{\infty} \langle \tilde{m}(1)|_b |\tilde{n}(2)\rangle_b A_n(t) - i\xi \sum_{n=0}^{\infty} \int_0^{\infty} \langle \tilde{m}(1)|_b |n\rangle_b C_{n,p,k}(t) dp, \quad (6b)$$

$$\dot{C}_{m,p,q}(t) = -i(\Delta_p + \Delta_q + m\omega_M)C_{m,p,q}(t) - i\xi \sum_{n=0}^{\infty} \langle m|_b |\tilde{n}(1)\rangle_b [B_{n,p}(t) + B_{n,q}(t)]. \quad (6c)$$

Here we point out that the transition rates associated with photon scattering processes are determined by the Franck-Condon factors $\langle \tilde{m}(2)|_b |\tilde{n}(1)\rangle_b$, $\langle \tilde{m}(1)|_b |\tilde{n}(2)\rangle_b$, $\langle \tilde{m}(1)|_b |n\rangle_b$, and $\langle m|_b |\tilde{n}(1)\rangle_b$, which can be calculated based on the relation [28]

$$\begin{aligned} & \langle m|_b e^{\beta_0(b^\dagger - b)} |n\rangle_b \\ &= \begin{cases} \sqrt{\frac{m!}{n!}} e^{-\frac{\beta_0^2}{2}} (-\beta_0)^{n-m} L_m^{n-m}(\beta_0^2), & n \geq m, \\ \sqrt{\frac{n!}{m!}} e^{-\frac{\beta_0^2}{2}} \beta_0^{m-n} L_n^{m-n}(\beta_0^2), & m > n, \end{cases} \quad (7) \end{aligned}$$

where $L_r^s(x)$ is the associated Laguerre polynomial.

III. TWO-PHOTON SCATTERING SOLUTION

Initially the cavity field is in the vacuum state and two photons are injected into the cavity. These two incident photons are prepared in a wave packet form outside the cavity. To facilitate analytic treatment by the Laplace transform, we examine the two-photon wave packet with Lorentzian spectrum. Without loss of generality, the initial state of the mirror is assumed to be number state $|n_0\rangle_b$. Once the solution in this case is found, the solution for general initial mirror states can be obtained accordingly by superposition. Explicitly, the initial condition is specified by $A_m(0) = 0$, $B_{m,k}(0) = 0$, and

$$C_{m,p,q}(0) = \left[\frac{\mathcal{N}\delta_{m,n_0}}{(\Delta_p - \delta_1 + i\epsilon)(\Delta_q - \delta_2 + i\epsilon)} + \delta_1 \leftrightarrow \delta_2 \right], \quad (8)$$

where $\delta_{j=1,2} = \omega_j - \omega_c$ (ω_j is the resonant frequency) and ϵ define the center detuning and spectral width of the two photons. The normalization constant \mathcal{N} is

$$\mathcal{N} = \frac{\epsilon}{\pi} \left(1 + \frac{4\epsilon^2}{(\delta_1 - \delta_2)^2 + (2\epsilon)^2} \right)^{-1/2}. \quad (9)$$

By using the Laplace transform, analytical solution of Eq. (6) subjected to the initial condition can be found (see Appendix). In the long-time limit when the scattering is completed and the two photons exit the cavity, the solution is given by: $A_{n_0,m}(\infty) = 0$, $B_{n_0,m,k}(\infty) = 0$,

and

$$C_{n_0,m,p,q}(\infty) = \mathcal{N}[(C_I + C_{II} + C_{III} + C_{IV}) + (\Delta_p \leftrightarrow \Delta_q)] e^{-i(\Delta_p + \Delta_q + m\omega_M)t} \quad (10)$$

Here, we add the subscript n_0 in $A_{n_0,m}(\infty)$, $B_{n_0,m,k}(\infty)$, and $C_{n_0,m,p,q}(\infty)$ to mark the mirror's initial state $|n_0\rangle_b$. The four transition amplitude components C_I , C_{II} , C_{III} , and C_{IV} are given by

$$\begin{aligned} C_I &= \frac{1}{(\Delta_p - \delta_1 + i\epsilon)} \frac{1}{(\Delta_q - \delta_2 + i\epsilon)} \delta_{m,n_0}, \\ C_{II} &= \sum_{n=0}^{\infty} \frac{-i\gamma_c F_{II}}{M_1 M_2 (\Delta_q - \delta_2 + i\epsilon)} + \delta_1 \leftrightarrow \delta_2, \\ C_{III} &= \sum_{n,n',l=0}^{\infty} \frac{-\gamma_c^2 F_{III}}{M_1 M_3 M_4 M_5} + \delta_1 \leftrightarrow \delta_2, \\ C_{IV} &= \sum_{n,n',l=0}^{\infty} \frac{-2\gamma_c^2 F_{IV}}{M_1 M_3 M_4 M_6} + \delta_1 \leftrightarrow \delta_2. \quad (11) \end{aligned}$$

where we have introduced F_{II-IV} to denote products of Franck-Condon factors

$$\begin{aligned} F_{II} &= \langle m|_b |\tilde{n}(1)\rangle_b \langle \tilde{n}(1)|_b |n_0\rangle_b, \\ F_{III} &= \langle m|_b |\tilde{n}(1)\rangle_b \langle \tilde{n}(1)|_b |n'\rangle_b \langle n'|_b |\tilde{l}(1)\rangle_b \langle \tilde{l}(1)|_b |n_0\rangle_b, \\ F_{IV} &= \langle m|_b |\tilde{n}(1)\rangle_b \langle \tilde{n}(1)|_b |\tilde{n}'(2)\rangle_b \langle \tilde{n}'(2)|_b |\tilde{l}(1)\rangle_b \langle \tilde{l}(1)|_b |n_0\rangle_b. \quad (12) \end{aligned}$$

In addition, the denominators in Eq. (11) are defined by

$$\begin{aligned} M_1 &= \Delta_p + \nu + (m - n)\omega_M + i\frac{\gamma_c}{2}, \\ M_2 &= \Delta_p - \delta_1 + (m - n_0)\omega_M + i\epsilon, \\ M_3 &= \Delta_p + \Delta_q - \delta_1 - \delta_2 + (m - n_0)\omega_M + 2i\epsilon, \\ M_4 &= \Delta_p + \Delta_q - \delta_1 + \nu + (m - l)\omega_M + i\frac{\gamma_c}{2} + i\epsilon, \\ M_5 &= \Delta_p - \delta_1 + (m - n')\omega_M + i\epsilon, \\ M_6 &= \Delta_p + \Delta_q + 4\nu + (m - n')\omega_M + i\gamma_c. \quad (13) \end{aligned}$$

From Eq. (13) we are able to determine the resonance conditions involved in the photon scattering process.

We point out that the four amplitudes C_{I-IV} correspond to four different physical processes in the two-photon scattering (see Fig. 2). The state transitions associated with these processes can be identified by F_{II-IV} .

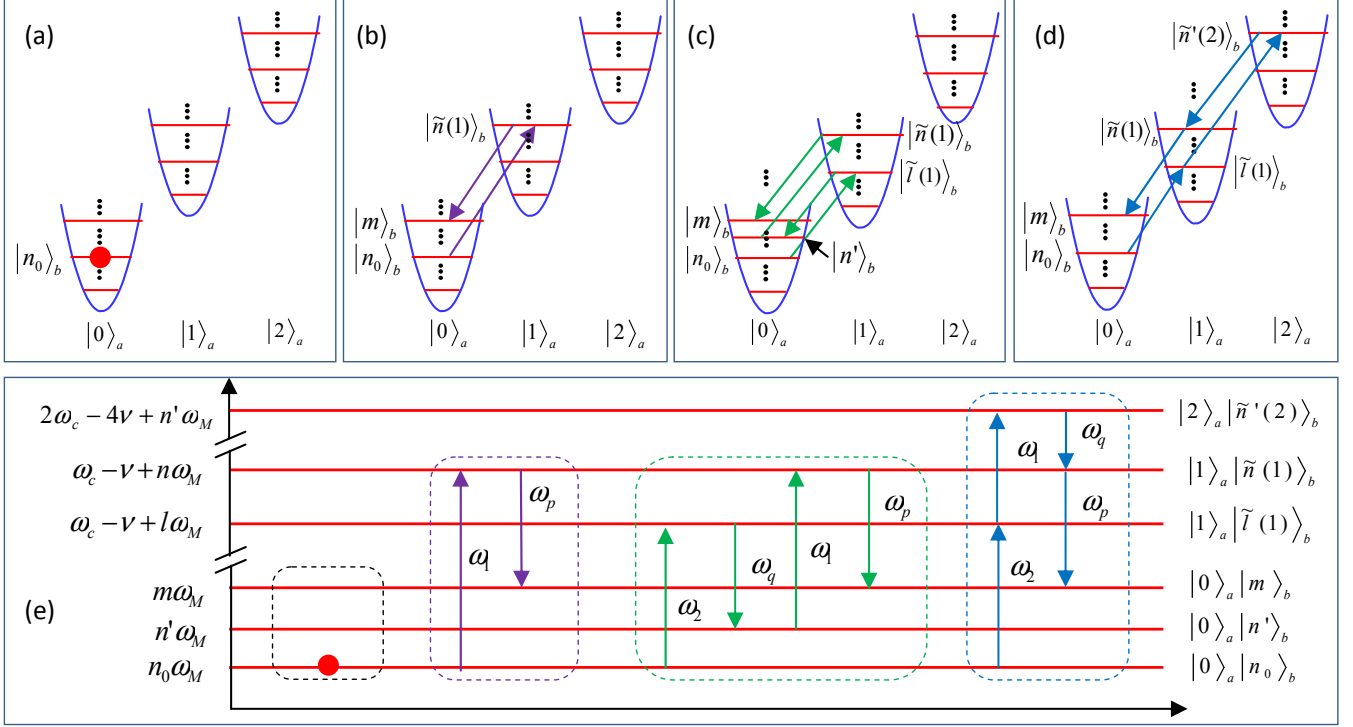


FIG. 2: (Color online) (a-d) Four types of transitions from states $|0\rangle_a|n_0\rangle_b$ to $|0\rangle_a|m\rangle_b$ of the optomechanical cavity in the two-photon scattering process. (e) The eigen-energies of these states involved in the four transition processes.

For the term C_I , it describes a direct two-photon reflection by the fixed end mirror without entering the cavity. Therefore the mirror state does not change, and the two reflected photons remain in the Lorentzian wave packet state [Fig. 2(a)].

The term C_{II} corresponds to the one-photon scattering and one-photon reflection process, i.e., just one photon enters the cavity and the other photon is reflected by the fixed end mirror. The entered photon induces the transition process $|0\rangle_a|n_0\rangle_b \rightarrow |1\rangle_a|\tilde{n}(1)\rangle_b \rightarrow |0\rangle_a|m\rangle_b$ [Fig. 2(b)], and such a process has the resonance conditions: $n_0\omega_M + \omega_1 = \omega_c - \nu + n\omega_M$ and $\omega_p = (\omega_c - \nu + n\omega_M) - m\omega_M$ [Fig. 2(e)], according to the poles of C_{II} , i.e., $\text{Re}(M_1) = 0$ and $\text{Re}(M_1 - M_2) = 0$.

The third term C_{III} can be interpreted as a sequential two-photon scattering process, in which the second photon enters the cavity after the first photon emitted out of the cavity. Such an interpretation is obtained from F_{III} that the maximum cavity photon number is one. In this case, the system experiences the following transitions $|0\rangle_a|n_0\rangle_b \rightarrow |1\rangle_a|\tilde{l}(1)\rangle_b \rightarrow |0\rangle_a|n'\rangle_b \rightarrow |1\rangle_a|\tilde{n}(1)\rangle_b \rightarrow |0\rangle_a|m\rangle_b$ [Fig. 2(c)]. As depicted in Fig. 2(e), the photon excitation processes are governed by $n_0\omega_M + \omega_2 = \omega_c - \nu + l\omega_M$ [i.e., $\text{Re}(M_4 - M_3) = 0$] and $n'\omega_M + \omega_1 = \omega_c - \nu + n\omega_M$ [$\text{Re}(M_1 - M_5) = 0$], and the frequencies of the two resonant emitted photons are $\omega_q = (\omega_c - \nu + l\omega_M) - n'\omega_M$ [$\text{Re}(M_4 - M_5) = 0$] and $\omega_p = (\omega_c - \nu + n\omega_M) - m\omega_M$ [$\text{Re}(M_1) = 0$].

The fourth term C_{IV} corresponds to a ‘genuine’ two-

photon process involving the interaction with two photons inside the cavity. This is revealed in F_{IV} having the states with two cavity photons. This is a kind of two-photon cascade scattering in which the system experiences the transitions $|0\rangle_a|n_0\rangle_b \rightarrow |1\rangle_a|\tilde{l}(1)\rangle_b \rightarrow |2\rangle_a|\tilde{n}'(2)\rangle_b \rightarrow |1\rangle_a|\tilde{n}(1)\rangle_b \rightarrow |0\rangle_a|m\rangle_b$ [Fig. 2(d)]. When the two photons are in the cavity, the mirror will experience an energy shift -4ν . This extra energy shift (and the phonon sidebands, as we will show below) provides the physical mechanism to create the photon blockade in the cavity. Due to the two-cavity-photon state is involved, the resonance conditions for the photon excitation processes are $n_0\omega_M + \omega_2 = \omega_c - \nu + l\omega_M$ [$\text{Re}(M_4 - M_3) = 0$] and $(\omega_c - \nu + l\omega_M) + \omega_1 = 2\omega_c - 4\nu + n'\omega_M$ [$\text{Re}(M_6 - M_4) = 0$]. In addition, the frequencies of the two emitted photons are $\omega_q = (2\omega_c - 4\nu + n'\omega_M) - (\omega_c - \nu + n\omega_M)$ [$\text{Re}(M_6 - M_1) = 0$] and $\omega_p = (\omega_c - \nu + n\omega_M) - m\omega_M$ [$\text{Re}(M_1) = 0$]. These resonance conditions can also be seen from Fig. 2(e).

The above analysis expatiated the physical picture for creation of two-photon correlation. In fact, after the scattering, the two photons will also entangle with the mirror. We can see this point by examining the scattering state of the system. We know from Eqs. (2) and (10) that, corresponding to the mirror's initial state $|n_0\rangle_b$, the long-time

state of the system is $|0\rangle_a \otimes |\Phi_{n_0}(\infty)\rangle$ with

$$|\Phi_{n_0}(\infty)\rangle = \sum_{m=0}^{\infty} \int_0^{\infty} dp \int_0^p dq C_{n_0,m,p,q}(\infty) |m\rangle_b |1_p, 1_q\rangle. \quad (14)$$

Physically, the cavity is in a vacuum in the long-time limit, and hence it decouples with the environment and the mirror. The state $|\Phi_{n_0}(\infty)\rangle$ is an entangled state involving these outside fields and the mirror. We can understand this entanglement from the dependence of the emitted photon modes on the mirror's final state $|m\rangle_b$. In the scattering process, the modes of the two emitted photons depend on the final state of the mirror [see Fig. 2(e)].

IV. TWO-PHOTON JOINT SPECTRUM

We know from the above section that the radiation-pressure coupling can induce photon correlation. We now show how to indicate qualitatively this correlation from the joint spectrum of the two scattered photons. Corresponding to the cases where the mirror is initially in a pure state $|\varphi\rangle_b = \sum_{n_0=0}^{\infty} c_{n_0} |n_0\rangle_b$ and a mixed state $\rho_b = \sum_{n_0=0}^{\infty} p_{n_0} |n_0\rangle_b \langle n_0|_b$, the joint spectrum functions [6] are defined by

$$S(\Delta_p, \Delta_q) = \sum_{m=0}^{\infty} \left| \sum_{n_0=0}^{\infty} c_{n_0} C_{n_0,m,p,q}(\infty) \right|^2, \quad (15a)$$

$$S(\Delta_p, \Delta_q) = \sum_{m=0}^{\infty} \sum_{n_0=0}^{\infty} p_{n_0} |C_{n_0,m,p,q}(\infty)|^2. \quad (15b)$$

In Fig. 3, we plot the two-photon joint spectrum $S(\Delta_p, \Delta_q)$ as a function of the frequencies Δ_p and Δ_q when the initial state of the mirror is $|0\rangle_b$. We firstly consider the case of $\beta_0 \ll 1$ so that it is reasonable to approximately expand the probability amplitude $C_{n_0,m,p,q}(\infty)$ up to the zero- and first-orders of β_0 , i.e., using the approximations

$$\begin{aligned} \langle m|_b e^{\beta_0(b^\dagger - b)} |n\rangle_b &\approx \delta_{m,n}, \\ \langle m|_b e^{\beta_0(b^\dagger - b)} |n\rangle_b &\approx \delta_{m,n} + \beta_0(\sqrt{n+1}\delta_{m,n+1} - \sqrt{n}\delta_{m,n-1}) \end{aligned} \quad (16)$$

in the zero- and first-order expansions, respectively. We note that the energy shift terms ν and 4ν in Eq. (13) are kept because $\nu = g_0\beta_0$ could be larger than γ_c even for small β_0 . Actually, the Kerr nonlinear energy shift $\nu(a^\dagger a)^2$ is responsible for the generation of photon correlation. For the zero-order expansion, the effect of the sidebands is completely canceled, and the present optomechanical system reduces to a Kerr nonlinear cavity with the Kerr parameter ν . When $\nu > \gamma_c$, two free photons scattered by the Kerr nonlinear cavity will be correlated [6]. This can be seen from the joint spectrum of

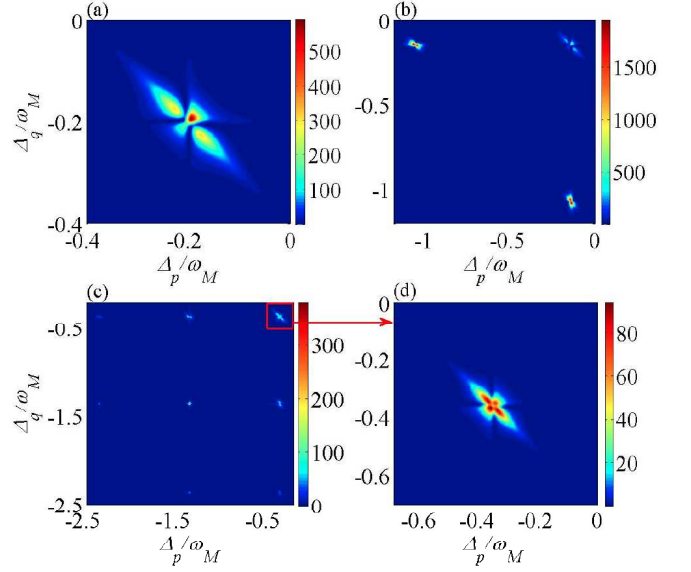


FIG. 3: (Color online) Plot of the two-photon joint spectrum $S(\Delta_p, \Delta_q)$ for the ground state $|0\rangle_b$ case. For a small $\beta_0 \ll 1$, we plot the spectrum by expanding the $C_{n_0,m,p,q}(\infty)$ up to (a) the zero-order ($\nu = 0.2$) and (b) the first-order ($\beta_0 = 0.4$) of β_0 . (c) For a large β_0 , the joint spectrum includes many sidebands ($\beta_0 = 0.6$). (d) The zoomed view of the peak with the center position $\Delta_p/\omega_M = \Delta_q/\omega_M = -0.36$ from the subfigure (c). Other parameters are: $\gamma_c/\omega_M = 0.1$, $\epsilon/\omega_M = 0.01$, and $\delta_1 = \delta_2 = -\nu$.

the two photons [Fig. 3(a)]. The two scattered photons are frequency anticorrelated with a probability concentrated along the line parallel to $\Delta_p + \Delta_q = 0$. For larger β_0 , the phonon sidebands will be involved in the spectrum. In the first-order expansion case, we can see two sideband peaks in the two directions of the joint spectrum. With the increasing of β_0 , more and more sidebands can be observed in the spectrum. In Fig. 3(c), we plot the joint spectrum in the single-photon strong coupling regime $\beta_0 = 0.6$. From the spectrum, we can see that the pattern of these sideband peaks is concentrated along the line parallel to $\Delta_p + \Delta_q = 0$. This point can be seen clearly from Fig. 3(d), which is a zoomed view of the peak with the center located at $\Delta_p = \Delta_q = -\nu$ in Fig. 3(c). We should emphasize that the joint spectrum is experimentally measurable by detecting the probability distribution of the two scattered photons.

V. PHOTON BLOCKADE IN CAVITY

In the previous section, we have studied the two-photon joint spectrum based on the long-time scattering solution. Actually, we can quantitatively study the photon correlation by calculating the second-order correlation function for cavity photons. However, we now need to consider the transient dynamics rather than the long-time dynamics of the system, because there are no pho-

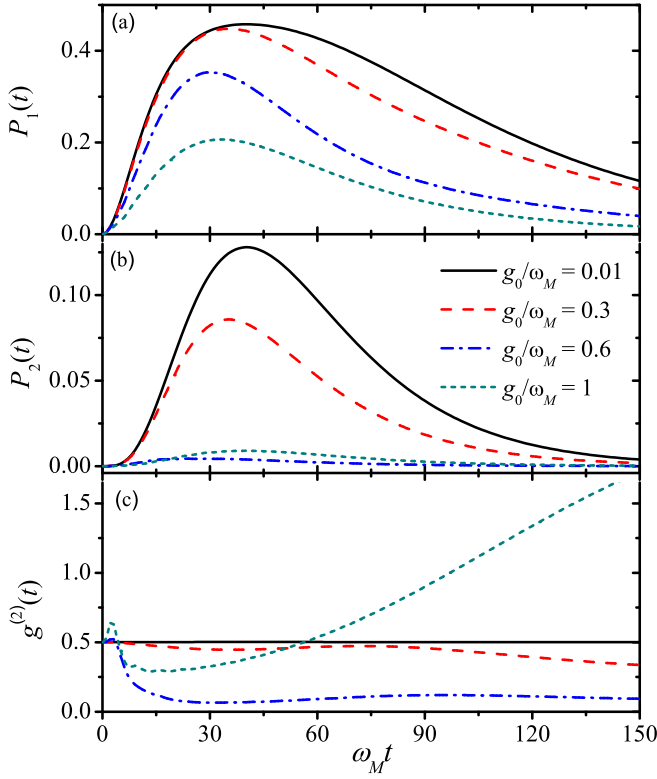


FIG. 4: (Color online) Evolution of (a) the single-photon probability $P_1(t)$ and (b) two-photon probability $P_2(t)$ in the cavity for various g_0 . (c) Equal-time second-order correlation function $g^{(2)}(t)$ vs the scaled time $\omega_M t$. Other parameters are: $\gamma_c/\omega_M = 0.1$, $\epsilon/\omega_M = 0.01$, $c_{n_0} = \delta_{n_0,0}$, and $\delta_1 = \delta_2 = -\nu$.

tons in the cavity in the long-time limit. In the following, we calculate the transient dynamics of the system based on the solution given in the Appendix. Corresponding to these two cases of initial states $|\varphi\rangle_b$ and ρ_b , the probabilities for finding one and two photons in the cavity can be obtained as

$$P_1(t) = \sum_{m=0}^{\infty} \int_0^{\infty} dk \left| \sum_{n_0=0}^{\infty} c_{n_0} B_{n_0,m,k}(t) \right|^2, \\ P_2(t) = \sum_{m=0}^{\infty} \left| \sum_{n_0=0}^{\infty} c_{n_0} A_{n_0,m}(t) \right|^2, \quad (17)$$

and

$$P_1(t) = \sum_{n_0=0}^{\infty} p_{n_0} \sum_{m=0}^{\infty} \int_0^{\infty} dk |B_{n_0,m,k}(t)|^2, \\ P_2(t) = \sum_{n_0=0}^{\infty} p_{n_0} \sum_{m=0}^{\infty} |A_{n_0,m}(t)|^2, \quad (18)$$

where $A_{n_0,m}(t)$ and $B_{n_0,m,k}(t)$ are obtained by making the inverse Laplace transform on Eqs. (A.10) and (A.11).

For the cavity field, the equal-time second-order correlation function is defined by [29]

$$g^{(2)}(t) \equiv \frac{\text{Tr}[\rho(t) a^\dagger a^\dagger a a]}{(\text{Tr}[\rho(t) a^\dagger a])^2}, \quad (19)$$

where $\rho(t)$ is the density matrix of the total system at time t . In terms of Eqs. (2), (17), and (18), Eq. (19) can be expressed as

$$g^{(2)}(t) = \frac{2P_2(t)}{[2P_2(t) + P_1(t)]^2}. \quad (20)$$

Photon blockade effect corresponds to $g^{(2)}(t) \ll 1$ [30], and the effect is measured by how small $g^{(2)}(t)$ is.

In what follows, we will study how the cavity photon statistics depends on the radiation-pressure coupling strength g_0 . In Fig. 4, we plot the time evolution of $P_1(t)$, $P_2(t)$, and $g^{(2)}(t)$ for various g_0 at $\delta_1 = \delta_2 = -\nu$, which corresponds to a single photon resonance [see Fig. 1(b)]. Here we assume that the initial state of the mirror is $|0\rangle_b$, i.e., $c_{n_0} = \delta_{n_0,0}$. We see that the probabilities $P_1(t)$ and $P_2(t)$ increase gradually from zero to a maximum value and then decrease to zero as time increases. At first glance, the maximum value of $P_2(t)$ is expected to decrease with the increase of g_0 because the two-photon detuning -2ν (i.e., the difference between the two-photon frequency shift -4ν and two photon's total energy -2ν) is proportional to g_0^2 , and therefore the photon blockade effect becomes stronger as g_0 increases. This trend is shown in the figure for g_0/ω_M from 0.01 to 0.6. However, we see that the dependence of $P_2(t)$ on g_0 is not monotonic due to the phonon sideband resonance effect. In fact, Fig. 4(c) shows that the photon blockade effect becomes weaker when $g_0/\omega_M = 1$. We can explain this feature by the fact when $g_0/\omega_M = 1$, the two photons can induce the resonant transitions $|0\rangle_a|0\rangle_b \rightarrow |1\rangle_a|\tilde{0}(1)\rangle_b$ and $|1\rangle_a|\tilde{0}(1)\rangle_b \rightarrow |2\rangle_a|\tilde{2}(2)\rangle_b$, and so the maximum of $P_2(t)$ in this case is larger than that for $g_0/\omega_M = 0.6$.

The oscillating feature of the correlation function $g^{(2)}$ as a function of g_0 was found in Ref. [17], which is based on an approximate steady state solution of a continuously driven system. In our case, our exact solution also indicates such a feature at transient times. This is shown in Fig. 5 in which the dependence of $g^{(2)}(t)$ on g_0 at a given time t_p is plotted. Here t_p is chosen when there are appreciable amount of photons inside the cavity. We can see clearly resonance peaks at specific values of g_0 . To explain the resonance, we note that when the frequencies of two photons are $\delta_1 = \delta_2 = -\nu$ used in the figure, resonant transitions $|0\rangle_a|0\rangle_b \rightarrow |2\rangle_a|\tilde{n}(2)\rangle_b$ are allowed if $-4\nu + n\omega_M = -2\nu$. This is the resonance condition allowing two photons to exist in the cavity at the same time. Specifically, the values of g_0 associated with these resonance peaks are located at

$$\frac{g_0}{\omega_M} = \sqrt{\frac{n}{2}}, \quad n = 0, 1, 2, \dots, \quad (21)$$

which are consistent with the locations of the resonance peaks in Fig. 5. We know from Eq. (21) that, with the

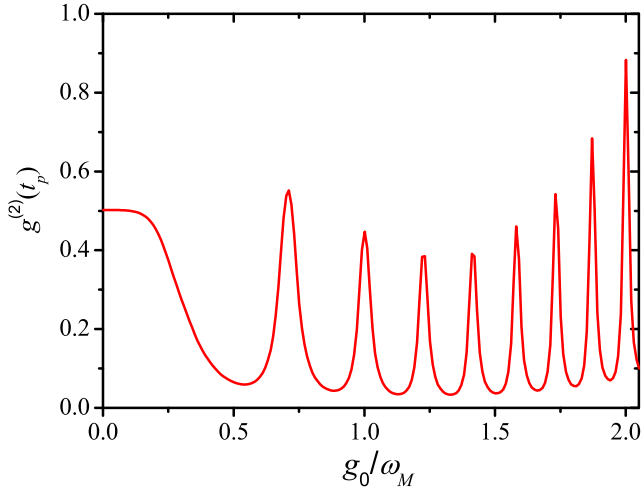


FIG. 5: (Color online) Plot of the equal-time second-order correlation function $g^{(2)}(t_p)$ at time $\omega_M t_p = 50$ vs the scaled coupling strength g_0/ω_M in the single-photon resonance case $\delta_1 = \delta_2 = -\nu$. Other parameters are the same as those in Fig. 4.

increasing of g_0 , the sideband modulation peaks become more and more dense.

The above discussions have considered the initial ground state of the mirror. It is interesting to ask how the $g^{(2)}(t)$ behaves when the mirror is in excited states initially. Suppose the initial state of the mirror is $|n\rangle_b$, then the system can undergo the transitions $|0\rangle_a|n\rangle_b \rightarrow |1\rangle_a|\tilde{n}(1)\rangle_b \rightarrow |2\rangle_a|\tilde{m}(2)\rangle_b$. Therefore, the Franck-Condon factors $\langle n|_b|\tilde{n}(1)\rangle_b$ and $\langle \tilde{n}(1)|_b|\tilde{m}(2)\rangle_b$ are important to determine the magnitude of $g^{(2)}(t)$. In Fig. 6, we illustrate this feature by considering a Fock state $|1\rangle_b$ as an initial state (blue dot dashed curve). For the parameters used in this figure, the relatively small Franck-Condon factor $\langle \tilde{1}(1)|_b|\tilde{1}(2)\rangle_b < \langle \tilde{0}(1)|_b|\tilde{0}(2)\rangle_b$ leads to a suppression of $P_2(t)$, and hence $g^{(2)}(t)$ can be substantially lower than that of the initial ground state (red dashed curve). In Fig. 6, we have also plotted the $g^{(2)}(t)$ (black solid curve) for the initial thermal state $\rho_b^{th}(\bar{n} = 1) = \sum_{n_0=0}^{\infty} 2^{-(n_0+1)}|n_0\rangle_b\langle n_0|_b$ (\bar{n} being the average thermal phonon number). We see that the $g^{(2)}(t)$ in this case is between those in the cases of $|0\rangle_b$ and $|1\rangle_b$ due to statistical mixture.

VI. CONCLUSION

In conclusion, we have studied analytically the two-photon scattering in a cavity optomechanical system. Under the Wigner-Weisskopf framework, we have obtained the exact transient solution of the system with the Laplace transform method. On one hand, the long-time solution reveals the detailed physical transitions for the two photons in the scattering process. This could help us to understand the physical mechanism to induce

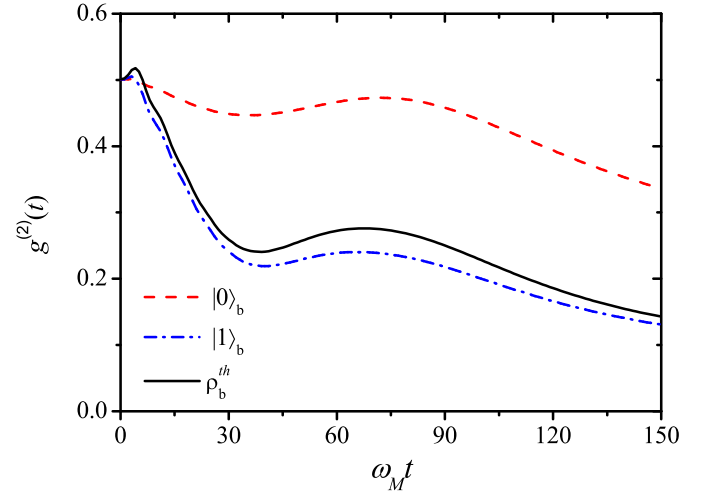


FIG. 6: (Color online) The second-order correlation function $g^{(2)}(t)$ vs the scaled time $\omega_M t$ when the mirror's initial state is Fock state $|1\rangle_b$ (blue dot dashed curve) and thermal state $\rho_b^{th}(\bar{n} = 1)$ (black solid curve). The ground state $|0\rangle_b$ case (red dashed curve) is presented as a reference. Other parameters are: $g_0/\omega_M = 0.3$, $\gamma_c/\omega_M = 0.1$, $\epsilon/\omega_M = 0.01$, and $\delta_1 = \delta_2 = -\nu$.

two-photon correlation. In addition, from the poles of these scattering amplitudes, we have obtained the resonance conditions of these transitions. In particular, the final state of the two photons is generally correlated in frequency space because of the frequency sum appearing in the denominator of the amplitudes C_{III} and C_{IV} . Based on the long-time solution, we have calculated the two-photon joint spectrum, which shows clear evidence for two-photon frequency anti-correlation. On the other hand, the transient dynamics of the equal-time second-order correlation function of the cavity photons has been calculated in order to address the photon blockade effect. We have found that the photon blockade effect can be induced by the optomechanical coupling. Besides, the correlation function has also been found to exhibit resonance peaks as a function of the optomechanical coupling strength, and we have determined the peak positions in Eq. (21) by a two-photon resonance condition.

Note added. We notice a related paper that appeared recently [31].

Acknowledgments

J. Q. Liao would like to thank J. F. Huang for technical support. This work is partially supported by a grant from the Research Grants Council of Hong Kong, Special Administrative Region of China (Project No. CUHK401810). J. Q. Liao is partially supported by Japan Society for the Promotion of Science (JSPS) Foreign Postdoctoral Fellowship No. P12503.

Appendix: Derivation of Eq. (10)

In this Appendix, we give a detailed derivation of the two-photon scattering solution in Eq. (10). By the Laplace transform $\tilde{f}(s) = \int_0^\infty f(t)e^{-st}dt$, Eq. (6) becomes

$$[s + i(m\omega_M - 4\nu)]\tilde{A}_m(s) = A_m(0) - i\sqrt{2}\xi \sum_{n=0}^{\infty} \int_0^\infty \langle \tilde{m}(2)|_b |\tilde{n}(1)\rangle_b \tilde{B}_{n,k}(s) dk, \quad (\text{A.1a})$$

$$[s + i(\Delta_k - \nu + m\omega_M)]\tilde{B}_{m,k}(s) = B_{m,k}(0) - i\sqrt{2}\xi \sum_{n=0}^{\infty} \langle \tilde{m}(1)|_b |\tilde{n}(2)\rangle_b \tilde{A}_n(s) - i\xi \sum_{n=0}^{\infty} \int_0^\infty \langle \tilde{m}(1)|_b |n\rangle_b \tilde{C}_{n,p,k}(s) dp, \quad (\text{A.1b})$$

$$[s + i(\Delta_p + \Delta_q + m\omega_M)]\tilde{C}_{m,p,q}(s) = C_{m,p,q}(0) - i\xi \sum_{n=0}^{\infty} \langle m|_b |\tilde{n}(1)\rangle_b [\tilde{B}_{n,p}(s) + \tilde{B}_{n,q}(s)], \quad (\text{A.1c})$$

where $A_m(0)$, $B_{m,k}(0)$, and $C_{m,p,q}(0)$ are the initial conditions, which are given in Eq. (8). From Eqs. (A.1a), (A.1c), and (8), we have

$$\tilde{A}_m(s) = \frac{-i\sqrt{2}\xi}{[s + i(m\omega_M - 4\nu)]} \sum_{n=0}^{\infty} \int_0^\infty \langle \tilde{m}(2)|_b |\tilde{n}(1)\rangle_b \tilde{B}_{n,k'}(s) dk', \quad (\text{A.2a})$$

$$\tilde{C}_{m,p,q}(s) = \frac{1}{[s + i(\Delta_p + \Delta_q + m\omega_M)]} \left(C_{m,p,q}(0) - i\xi \sum_{n=0}^{\infty} \langle m|_b |\tilde{n}(1)\rangle_b [\tilde{B}_{n,p}(s) + \tilde{B}_{n,q}(s)] \right), \quad (\text{A.2b})$$

Substitution of Eqs. (A.2a) and (A.2b) into Eq. (A.1b) leads to

$$\begin{aligned} & \left[s + \frac{\gamma_c}{2} + i(\Delta_k - \nu + m\omega_M) \right] \tilde{B}_{m,k}(s) \\ &= - \int_0^\infty \sum_{l,n=0}^{\infty} \left(\frac{2\xi^2 \langle \tilde{m}(1)|_b |\tilde{n}(2)\rangle_b \langle \tilde{n}(2)|_b |\tilde{l}(1)\rangle_b}{[s + i(n\omega_M - 4\nu)]} + \frac{\xi^2 \langle \tilde{m}(1)|_b |n\rangle_b \langle n|_b |\tilde{l}(1)\rangle_b}{[s + i(\Delta_p + \Delta_k + n\omega_M)]} \right) \tilde{B}_{l,p}(s) dp \\ & \quad + 2i\pi\xi\mathcal{N} \langle \tilde{m}(1)|_b |n_0\rangle_b \left(\frac{1}{[\Delta_k + \delta_1 + n_0\omega_M - i(s + \epsilon)](\Delta_k - \delta_2 + i\epsilon)} + \delta_1 \leftrightarrow \delta_2 \right), \end{aligned} \quad (\text{A.3})$$

where $\gamma_c = 2\pi\xi^2$ is the cavity-field decay rate. We introduce a new variable $\tilde{F}_{m,k}(s)$ by

$$\tilde{B}_{m,k}(s) = \frac{2\pi i\xi\mathcal{N} \langle \tilde{m}(1)|_b |n_0\rangle_b}{[s + \frac{\gamma_c}{2} + i(\Delta_k - \nu + m\omega_M)]} \left(\frac{1}{[\Delta_k + \delta_1 + n_0\omega_M - i(s + \epsilon)](\Delta_k - \delta_2 + i\epsilon)} + \delta_1 \leftrightarrow \delta_2 \right) [1 + \tilde{F}_{m,k}(s)]. \quad (\text{A.4})$$

Then the equation for $\tilde{F}_{m,k}(s)$ is obtained as

$$\begin{aligned} & \left(\frac{\langle \tilde{m}(1)|_b |n_0\rangle_b}{[\Delta_k + \delta_1 + n_0\omega_M - i(s + \epsilon)](\Delta_k - \delta_2 + i\epsilon)} + \delta_1 \leftrightarrow \delta_2 \right) \tilde{F}_{m,k}(s) \\ &= - \int_0^\infty \sum_{l,n=0}^{\infty} \left(\frac{2\xi^2 \langle \tilde{m}(1)|_b |\tilde{n}(2)\rangle_b \langle \tilde{n}(2)|_b |\tilde{l}(1)\rangle_b}{[s + i(n\omega_M - 4\nu)]} + \frac{\xi^2 \langle \tilde{m}(1)|_b |n\rangle_b \langle n|_b |\tilde{l}(1)\rangle_b}{[s + i(\Delta_p + \Delta_k + n\omega_M)]} \right) \frac{\langle \tilde{l}(1)|_b |n_0\rangle_b}{[s + \frac{\gamma_c}{2} + i(\Delta_p - \nu + l\omega_M)]} \\ & \quad \times \left(\frac{1}{[\Delta_p + \delta_1 + n_0\omega_M - i(s + \epsilon)](\Delta_p - \delta_2 + i\epsilon)} + \delta_1 \leftrightarrow \delta_2 \right) \tilde{F}_{l,p}(s) dp + S_1, \end{aligned} \quad (\text{A.5})$$

where

$$\begin{aligned} S_1 &= \frac{1}{[\delta_1 + \delta_2 + n_0\omega_M - i(s + 2\epsilon)]} \sum_{l,n=0}^{\infty} \left[\left(\frac{2\gamma_c \langle \tilde{m}(1)|_b |\tilde{n}(2)\rangle_b \langle \tilde{n}(2)|_b |\tilde{l}(1)\rangle_b \langle \tilde{l}(1)|_b |n_0\rangle_b}{[s + i(n\omega_M - 4\nu)][\delta_1 - \nu + l\omega_M - i(s + \epsilon + \frac{\gamma_c}{2})]} \right. \right. \\ & \quad \left. \left. - \frac{i\gamma_c \langle \tilde{m}(1)|_b |n\rangle_b \langle n|_b |\tilde{l}(1)\rangle_b \langle \tilde{l}(1)|_b |n_0\rangle_b}{[\delta_1 + \Delta_k + n\omega_M - i(\epsilon + s)][\delta_1 - \nu + l\omega_M - i(s + \epsilon + \frac{\gamma_c}{2})]} \right) + (\delta_1 \leftrightarrow \delta_2) \right]. \end{aligned} \quad (\text{A.6})$$

By introducing a new variable $x_m(s)$

$$\tilde{F}_{m,k}(s) = \left(\frac{\langle \tilde{m}(1)|_b | n_0 \rangle_b}{(\Delta_k - \delta_2 + i\epsilon)[\Delta_k + \delta_1 + n_0\omega_M - i(s + \epsilon)]} + \delta_1 \leftrightarrow \delta_2 \right)^{-1} [S_1 + x_m(s)], \quad (\text{A.7})$$

we obtain the equation for $x_m(s)$ as follows:

$$x_m(s) + \sum_{l,n=0}^{\infty} \frac{\gamma_c \langle \tilde{m}(1)|_b | \tilde{n}(2) \rangle_b \langle \tilde{n}(2)|_b | \tilde{l}(1) \rangle_b}{[s + i(n\omega_M - 4\nu)]} x_l(s) = - \sum_{l,n=0}^{\infty} \frac{2\gamma_c^2 \langle \tilde{m}(1)|_b | \tilde{n}(2) \rangle_b \langle \tilde{n}(2)|_b | \tilde{l}(1) \rangle_b \langle \tilde{l}(1)|_b | n_0 \rangle_b}{[\delta_1 + \delta_2 + n_0\omega_M - i(s + 2\epsilon)][s + i(n\omega_M - 4\nu)]^2} \times \left(\frac{1}{[\delta_1 - \nu + l\omega_M - i(s + \epsilon + \frac{\gamma_c}{2})]} + \delta_1 \leftrightarrow \delta_2 \right), \quad (\text{A.8})$$

The solution of Eq. (A.8) can be found as

$$x_m(s) = \sum_{l,n=0}^{\infty} \frac{2\gamma_c^2}{[s + \gamma_c + i(n\omega_M - 4\nu)]} \frac{\langle \tilde{m}(1)|_b | \tilde{n}(2) \rangle_b \langle \tilde{n}(2)|_b | \tilde{l}(1) \rangle_b \langle \tilde{l}(1)|_b | n_0 \rangle_b}{[s + 2\epsilon + i(\delta_1 + \delta_2 + n_0\omega_M)][s + i(n\omega_M - 4\nu)]} \times \left(\frac{1}{[(s + \epsilon + \frac{\gamma_c}{2}) + i(\delta_1 - \nu + l\omega_M)]} + \delta_1 \leftrightarrow \delta_2 \right). \quad (\text{A.9})$$

Then by Eqs. (A.2a), (A.2b), (A.4), (A.7), and (A.9), we can obtain

$$\begin{aligned} \tilde{A}_m(s) &= \frac{2\sqrt{2}\pi\mathcal{N}\gamma_c}{[s + 2\epsilon + i(\delta_1 + \delta_2 + n_0\omega_M)][s + \gamma_c + i(m\omega_M - 4\nu)]} \sum_{n=0}^{\infty} \left(\frac{\langle \tilde{m}(2)|_b | \tilde{n}(1) \rangle_b \langle \tilde{n}(1)|_b | n_0 \rangle_b}{[s + \epsilon + \frac{\gamma_c}{2} + i(\delta_1 - \nu + n\omega_M)]} + \delta_1 \leftrightarrow \delta_2 \right) \\ \tilde{B}_{m,k}(s) &= - \frac{2\pi\xi\mathcal{N}\langle \tilde{m}(1)|_b | n_0 \rangle_b}{[s + \frac{\gamma_c}{2} + i(\Delta_k - \nu + m\omega_M)]} \left(\frac{1}{(\Delta_k - \delta_2 + i\epsilon)} \frac{1}{[s + \epsilon + i(\Delta_k + \delta_1 + n_0\omega_M)]} + \delta_1 \leftrightarrow \delta_2 \right) \\ &\quad - \sum_{l,n=0}^{\infty} \frac{4\pi i\xi\mathcal{N}\gamma_c \langle \tilde{m}(1)|_b | \tilde{n}(2) \rangle_b \langle \tilde{n}(2)|_b | \tilde{l}(1) \rangle_b \langle \tilde{l}(1)|_b | n_0 \rangle_b}{[s + \frac{\gamma_c}{2} + i(\Delta_k - \nu + m\omega_M)][s + 2\epsilon + i(\delta_1 + \delta_2 + n_0\omega_M)]} \\ &\quad \times \frac{1}{[s + \gamma_c + i(n\omega_M - 4\nu)]} \left(\frac{1}{[s + \epsilon + \frac{\gamma_c}{2} + i(\delta_1 - \nu + l\omega_M)]} + \delta_1 \leftrightarrow \delta_2 \right) \\ &\quad - \sum_{l,n} \frac{2\pi i\xi\mathcal{N}\gamma_c \langle \tilde{m}(1)|_b | n \rangle_b \langle n|_b | \tilde{l}(1) \rangle_b \langle \tilde{l}(1)|_b | n_0 \rangle_b}{[s + \frac{\gamma_c}{2} + i(\Delta_k - \nu + m\omega_M)][s + 2\epsilon + i(\delta_1 + \delta_2 + n_0\omega_M)]} \\ &\quad \times \left(\frac{1}{[s + \epsilon + i(\Delta_k + \delta_1 + n\omega_M)][s + \epsilon + \frac{\gamma_c}{2} + i(\delta_1 - \nu + l\omega_M)]} + \delta_1 \leftrightarrow \delta_2 \right), \quad (\text{A.11}) \end{aligned}$$

$$\begin{aligned} \tilde{C}_{m,p,q}(s) &= \frac{\mathcal{N}}{[s + i(\Delta_p + \Delta_q + m\omega_M)]} \left[\frac{1}{(\Delta_p - \delta_1 + i\epsilon)} \frac{1}{(\Delta_q - \delta_2 + i\epsilon)} \delta_{m,n_0} + \sum_{n=0}^{\infty} \frac{i\gamma_c \langle m|_b | \tilde{n}(1) \rangle_b \langle \tilde{n}(1)|_b | n_0 \rangle_b}{[s + \frac{\gamma_c}{2} + i(\Delta_p - \nu + n\omega_M)]} \right. \\ &\quad \times \left(\frac{1}{[s + \epsilon + i(\Delta_p + \delta_1 + n_0\omega_M)]} \frac{1}{(\Delta_p - \delta_2 + i\epsilon)} + \delta_1 \leftrightarrow \delta_2 \right) \\ &\quad - \sum_{n,n',l=0}^{\infty} \frac{\gamma_c^2 \langle m|_b | \tilde{n}(1) \rangle_b \langle \tilde{n}(1)|_b | n' \rangle_b \langle n'|_b | \tilde{l}(1) \rangle_b \langle \tilde{l}(1)|_b | n_0 \rangle_b}{[s + 2\epsilon + i(\delta_1 + \delta_2 + n_0\omega_M)][s + \frac{\gamma_c}{2} + i(\Delta_p - \nu + n\omega_M)]} \\ &\quad \times \left(\frac{1}{[s + \epsilon + \frac{\gamma_c}{2} + i(\delta_1 - \nu + l\omega_M)]} \frac{1}{[s + \epsilon + i(\Delta_p + \delta_1 + n'\omega_M)]} + \delta_1 \leftrightarrow \delta_2 \right) \\ &\quad - \sum_{n,n',l=0}^{\infty} \frac{2\gamma_c^2 \langle m|_b | \tilde{n}(1) \rangle_b \langle \tilde{n}(1)|_b | \tilde{n}'(2) \rangle_b \langle \tilde{n}'(2)|_b | \tilde{l}(1) \rangle_b \langle \tilde{l}(1)|_b | n_0 \rangle_b}{[s + 2\epsilon + i(\delta_1 + \delta_2 + n_0\omega_M)][s + \gamma_c + i(n'\omega_M - 4\nu)][s + \frac{\gamma_c}{2} + i(\Delta_p - \nu + n\omega_M)]} \\ &\quad \times \left(\frac{1}{[s + \epsilon + \frac{\gamma_c}{2} + i(\delta_1 - \nu + l\omega_M)]} + \delta_1 \leftrightarrow \delta_2 \right) \left. \right] + \Delta_p \leftrightarrow \Delta_q. \quad (\text{A.12}) \end{aligned}$$

The transient solution of these probability amplitudes $A_{n_0,m}(t)$, $B_{n_0,m,k}(t)$, and $C_{n_0,m,p,q}(t)$ can be obtained by the inverse Laplace transform. Here we add the subscript n_0 in the transient solution to mark the mirror's initial state $|n_0\rangle_b$. The corresponding long-time solution is given in Eq. (10).

-
- [1] A. Imamoglu, H. Schmidt, G. Woods, and M. Deutsch, Phys. Rev. Lett. **79**, 1467 (1997).
 - [2] K. M. Birnbaum, A. Boca, R. Miller, A. D. Boozer, T. E. Northup, and H. J. Kimble, Nature (London) **436**, 87 (2005).
 - [3] K. Kojima, H. F. Hofmann, S. Takeuchi, and K. Sasaki, Phys. Rev. A **68**, 013803 (2003).
 - [4] J. T. Shen and S. Fan, Phys. Rev. Lett. **98**, 153003 (2007); Phys. Rev. A **76**, 062709 (2007).
 - [5] T. Shi and C. P. Sun, Phys. Rev. B **79**, 205111 (2009); T. Shi, S. Fan, and C. P. Sun, Phys. Rev. A **84**, 063803 (2011).
 - [6] J. Q. Liao and C. K. Law, Phys. Rev. A **82**, 053836 (2010).
 - [7] D. Roy, Phys. Rev. B **81**, 155117 (2010); Phys. Rev. Lett. **106**, 053601 (2011).
 - [8] P. Kolchin, R. F. Oulton, and X. Zhang, Phys. Rev. Lett. **106**, 113601 (2011).
 - [9] H. Zheng, D. J. Gauthier, and H. U. Baranger, Phys. Rev. A **85**, 043832 (2012).
 - [10] A. J. Hoffman, S. J. Srinivasan, S. Schmidt, L. Spietz, J. Aumentado, H. E. Türeci, and A. A. Houck, Phys. Rev. Lett. **107**, 053602 (2011).
 - [11] T. J. Kippenberg and K. J. Vahala, Science **321**, 1172 (2008).
 - [12] F. Marquardt and S. M. Girvin, Physics **2**, 40 (2009).
 - [13] I. Favero and K. Karrai, Nature Photonics **3**, 201 (2009).
 - [14] S. Mancini, V. I. Manko, and P. Tombesi, Phys. Rev. A **55**, 3042 (1997).
 - [15] S. Bose, K. Jacobs, and P. L. Knight, Phys. Rev. A **56**, 4175 (1997).
 - [16] Z. R. Gong, H. Ian, Y. X. Liu, C. P. Sun, and F. Nori, Phys. Rev. A **80**, 065801 (2009).
 - [17] P. Rabl, Phys. Rev. Lett. **107**, 063601 (2011).
 - [18] W. Marshall, C. Simon, R. Penrose, and D. Bouwmeester, Phys. Rev. Lett. **91**, 130401 (2003).
 - [19] T. Hong, H. Yang, H. Miao, and Y. Chen, e-print arXiv:1110.3348.
 - [20] A. Nunnenkamp, K. Børkje, and S. M. Girvin, Phys. Rev. Lett. **107**, 063602 (2011).
 - [21] J. Q. Liao, H. K. Cheung, and C. K. Law, Phys. Rev. A **85**, 025803 (2012).
 - [22] A. Nunnenkamp, K. Børkje, and S. M. Girvin, Phys. Rev. A **85**, 051803 (2012).
 - [23] J. Qian, A. A. Clerk, K. Hammerer, and F. Marquardt, Phys. Rev. Lett. **109**, 253601 (2012).
 - [24] S. Gupta, K. L. Moore, K. W. Murch, and D. M. Stamper-Kurn, Phys. Rev. Lett. **99**, 213601 (2007).
 - [25] F. Brennecke, S. Ritter, T. Donner, and T. Esslinger, Science **322**, 235 (2008).
 - [26] M. Eichenfield, J. Chan, R. M. Camacho, K. J. Vahala, and O. Painter, Nature (London) **462**, 78 (2009).
 - [27] A. Kronwald, M. Ludwig, and F. Marquardt, Phys. Rev. A **87**, 013847 (2013).
 - [28] F. A. M. de Oliveira, M. S. Kim, P. L. Knight, and V. Buzek, Phys. Rev. A **41**, 2645 (1990).
 - [29] R. Loudon, *The Quantum Theory of Light* (Oxford University Press, New York, 2000).
 - [30] M. J. Werner and A. Imamoglu, Phys. Rev. A **61**, 011801(R) (1999).
 - [31] X. W. Xu, Y. J. Li, and Y. X. Liu, Phys. Rev. A **87**, 025803 (2013).